ISSN 0021-3640, JETP Letters, 2007, Vol. 85, No. 12, pp. 649–654. © Pleiades Publishing, Ltd., 2007.
Original Russian Text © S.N. Martynov, A.D. Balaev, 2007, published in Pis'ma v Zhurnal Éksperimental'noĭ i Teoreticheskoĭ Fiziki, 2007, Vol. 85, No. 12, pp. 785–790.

Frustration Mechanism of Formation of a Helical Magnetic Structure in the CuB_2O_4 Two-Subsystem Antiferromagnet

S. N. Martynov[a] and A. D. Balaev[b]

[a] *Siberian Federal University, Krasnoyarsk, 660041 Russia*
e-mail: unonav@iph.krasn.ru
[b] *Kirensky Institute of Physics, Siberian Division, Russian Academy of Sciences, Akademgorodok, Krasnoyarsk, 660036 Russia*

Received May 3, 2007; in final form, May 16, 2007

A new mechanism is proposed for forming an incommensurate magnetic structure of the transverse helix type owing to the removal of frustration through intersubsystem exchange in a two-subsystem antiferromagnet. The symmetry analysis of the distribution of the Dzyaloshinskii–Moriya interaction and comparison with the experimental data on the field dependence of magnetization indicate that antisymmetric exchange and competition between symmetric exchanges cannot be responsible for forming a helical magnetic structure in CuB_2O_4.

PACS numbers: 75.10.Jm, 75.50.Ee, 75.50.-y

DOI: 10.1134/S0021364007120132

Frustrated magnetic systems have been investigated for a long time in the physics of phase transitions and critical phenomena [1, 2]. This interest is associated with an additional degree of freedom appearing due to the degeneration of the classical ground state. The most well-known example is the 120-degree orientation of the spins, which appears in the triangular frustrated antiferromagnet and gives rise to chirality as an additional degree of freedom and to a new class of critical exponents [3]. As a result, the nature of the phase transition in the frustrated systems can significantly differ from similar transformations in unfrustrated magnets.

The magnetic properties of copper metaborate (CuB_2O_4) have been analyzed for the past several years in many works [4–11]. This interest is primarily stimulated by the existence of an incommensurate magnetic structure in this compound. However, the mechanism of formation of this structure, i.e., interactions responsible for incommensurability, remains unknown. The incommensurate magnetic structure is formed due to the competition between magnetic, primarily exchange, interactions. The following two mechanisms are usually considered: first, the competition between symmetric exchanges (most often, between the first and second nearest magnetic neighbors), the so-called exchange mechanism, and, second, the competition between symmetric and antisymmetric exchanges, which is the relativistic mechanism [12]. In view of the relative smallness of the antisymmetric exchange (Dzyaloshinskii–Moriya interaction [13]), the long-period incommensurate magnetic structure is usually formed in the latter case. Since the center of inversion is absent in the crystal structure of CuB_2O_4, most authors attribute the appearance of the incommensurate magnetic structure to the second mechanism. The exchange interactions in CuB_2O_4 occur through the boron–oxygen tetrahedra, which leads to the large length and diversity of exchange bonds, including possible competing bonds. This mechanism was also discussed as an alternating or additional mechanism in [14, 15]. In the magnets consisting of two or more different magnetic subsystems, the class of possible interactions responsible for the formation of the incommensurate magnetic structure expands significantly. Both mechanisms can be present in each subsystem and in intersubsystem interactions. The aim of this work is to reveal the cause of the formation of the incommensurate magnetic structure in CuB_2O_4.

The crystal structure of CuB_2O_4 belongs to the space group $I\bar{4}2d$, is well studied, and was described in [16, 5, 9] (see Fig. 1). Its feature is the presence of two nonequivalent sites of the Cu^{2+} ions and, as a result, the presence of qualitatively different exchange interactions both inside each magnetic subsystem and between the subsystems. The antiferromagnetic exchange interaction between the ions in the 4b site (CuA) is the strongest interaction and forms the long-range antiferromagnetic order in this "strong" subsystem at $T_N = 20$ K. Exchange bonds forming double zigzag magnetic chains along the tetragonal **c** axis exist inside the "weak" subsystem of copper ions at the 8b (CuB) site [14]. The exchange interactions between the subsystems are completely frustrated: each moment of CuB in the ordered phase at $T < T_N$ is identically coupled with the spins of both antiferromagnetic CuA sublattices. Exchange paths, which can be frustrated under the assumption of antiferromagnetic ordering inside the

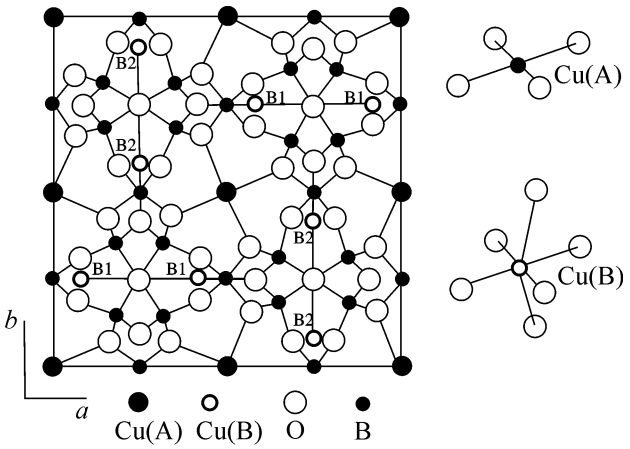

Fig. 1. Crystal structure of CuB_2O_4.

chains, also exist between the chains of subsystem B. All these exchanges proceed through the hybridized *s–p* orbitals of boron–oxygen complexes, i.e., single or double Cu–O–B–O–Cu paths of various configurations.

The temperature–field magnetic phase diagram [11] at $T < 20$ K has the commensurate weak ferromagnetic phase in high fields and two modulated phases in the fields lower than the critical field. The long-periodic structure at 9.5 K < T < 20 K is an open problem, whereas a helical incommensurate magnetic structure with the wave vector $\mathbf{k} \parallel \mathbf{c}$ and transverse polarization is formed below $T_s = 9.5$ K [9]. Near the transition to the helical phase, T_s, in addition to the main peak of the incommensurate magnetic structure in neutron scattering in zero field, weaker satellite peaks are also observed, indicating a weak modulation of the helix, the so-called "soliton lattice" [6]. As the temperature increases, the wave vector of the helix increases continuously from zero at T_s to 0.15 rlu at $T \approx 2$ K. The phenomenological analysis [10] shows that such a behavior of the wave vector of the structure can be described in terms of the thermodynamic potential and Lifshitz invariant constructed on two two-component order parameters including the magnetic modes of both subsystems. The temperature dependence of the average magnetization of subsystems is of primary importance for understanding of the temperature and field evolution of the magnetic structure. At $T < 10$ K, the moment at the site of the strong subsystem A is close to the separation, $M_a = g\mu_B S_A > 0.9\mu_B$, even in zero field $H = 0$. The magnetic moment at the site of the weak subsystem B in zero field is not saturated down to accessible low temperatures and is equal to $M_B \sim 0.2\mu_B$ and $0.5\mu_B$ at $T = 12$ and 2 K, respectively [9]. This property can indicate both the smallness of the exchange interactions involving the moments of subsystem B and the quasi-low-dimensional character of exchange in this subsystem. The existence of the low-energy branch in the spectrum of inelastic neutron scattering only for $\mathbf{k} \parallel \mathbf{c}$ [14] also indicates the dominant role of exchange along the double chains among the interactions in subsystem B. The second factor directly affecting the formation of the transverse helix is the orientation of the magnetic moments of the subsystems. Moment subsystem A is an easy-plane antiferromagnet with a weak ferromagnetic moment in a tetragonal plane in the commensurate high-field phase $H > H_c(T)$. The moments of its sublattices in the absence of the field primarily lie in the tetragonal plane with small deviations toward the **c** axis. On the contrary, the moments S_B at $T = 12$ K are oriented almost exactly along the **c** axis and undergo the orientation transition when the temperature is decreased to 2 K to the angular phase with an angle of about 60° between the direction of the moments and the **c** axis in the commensurate high-field phase [9].

Depending on the symmetry transformations of a pair of interacting spins, the antisymmetric interaction can result either in weak ferromagnetism or in the helix structure. For the appearance of the transverse helix with the propagation vector along the tetragonal axis $\mathbf{k} \parallel \mathbf{c}$, the component of the pseudovector **D** of this exchange along this axis must exist. For this reason, we analyze only this pseudovector component. In terms of the subscripts $i \in A$, $j \in B1$, and $j' \in B2$ along the **c** axis, the Hamiltonians for the exchange inside subsystem A and between the subsystems have the form

$$H_D^A = \sum_i \mathbf{D}_i^A [\mathbf{S}_i \times \mathbf{S}_{i+1}],$$
$$H_D^{AB} = \sum_{lij(j')} \mathbf{D}_{lij(j')}^{AB} [\mathbf{S}_i \times \mathbf{S}_{j(j')}]. \quad (1)$$

Here, the subscript $l = 1, 2, 3$ refers to three different paths of exchange interactions between the subsystems. Figure 2 shows exchange paths inside subsystem A and interaction paths between neighbors A and B nearest in the tetragonal axis. Both exchanges are equivalent: pairs of interacting spins along the tetragonal axis ($i \longrightarrow i + 1$ or $j \longrightarrow j'$ in the first and second cases, respectively) are transformed to each other by means of the rotation of the fourth-order axes $\bar{4}_3^1$ and $\bar{4}_3^3$ together with the inversion $\bar{I}$ with respect to the central spin A. As a result, $\mathbf{D}_i^A = (-1)^i \mathbf{D}^A$ and $\mathbf{D}_{lij}^{AB} = \mathrm{sgn}(i - j(j'))\mathbf{D}_l^{AB}$. These exchanges give rise to the alternating of the inclinations of the magnetic moments along the **c** axis and, as a result, to weak ferromagnetism.

The next group of the exchange inside the double chains of subsystem B,

$$H_D^B = \sum_{nj} \mathbf{D}_{nj}^B [\mathbf{S}_j \times \mathbf{S}_{j+n}], \quad (2)$$

where $n = 1$ and 2 refer to the exchange between the first and second nearest neighbors in the chain, respectively, is transformed by means of the rotation about the second-order axes 4_1^2 and 4_2^2 lying in the tetragonal plane and passing through the ions B. This leads both to the subscript change $j + n \longleftrightarrow j - n$ and to a change in the sign of the pseudovector $\mathbf{D}$, which finally reduces to the second type of the antisymmetric exchange $\mathbf{D}_{nj}^B = \mathbf{D}_n^B$. Thus, the helix structure can be formed inside the chains of subsystem B. However, different chains B1–B1 and B2–B2 (see Fig. 1) are transformed to each other by means of the transition about the fourth-order axis with inversion, which is the same as for the first-group exchanges. In this case, the order of the indices in the neighboring chains changes: $j + 1 \longleftrightarrow j' - 1$, but the pseudovector conserves its sign. As a result, the signs of the pseudovectors in neighboring chains when following in the same direction in the indices j and j' are opposite: $\mathbf{D}_n^{B1} - \mathbf{D}_n^{B2}$. Thus, the general double degeneration is recovered and the symmetry of the order parameter increases to $Z_2 \times SO(2)$. Therefore, the formation of a common simple helix with one vector $\mathbf{k}$ becomes impossible in the presence of the antisymmetric exchange with the longitudinal components $\mathbf{D}_n^{B1,2}$. In this case, the antisymmetric exchange can lead either to a more complex incommensurate magnetic structure or to the modulation of the simple helix formed through other mechanisms. The antisymmetric exchange that is possible between spins B of different chains also has the alternating sign of the longitudinal component.

The Hamiltonian of the model

$$H = h\left(\sum_i \mathbf{S}_i^A + \sum_j \mathbf{S}_j^B\right) + J^A \sum_{ii'} \mathbf{S}_i \mathbf{S}_i' + J_1^B \sum_j \mathbf{S}_j^B \mathbf{S}_{j+1}^B + J_2^B \sum_j \mathbf{S}_j^B \mathbf{S}_{j+2}^B + \sum_{l=1}^{3} J_l^{AB} \sum_{ij} \mathbf{S}_i^A \mathbf{S}_j^B \quad (3)$$

includes the interaction energy with the external field, isotropic exchange inside subsystem A, two exchanges with the first and second nearest neighbors in the double chains of subsystem B, and three intersubsystem exchanges. Since the main attention is focused on the analysis of the behavior at the boundary of the phase diagram (near the transition to the incommensurate phase) in comparatively high fields, the effect of other anisotropic interactions at this stage is disregarded. Since the formation of a simple, i.e., uniform helix is analyzed, the local orientation of the magnetic moments in the coordinate system rotating when displacing along the tetragonal axis depends only on three

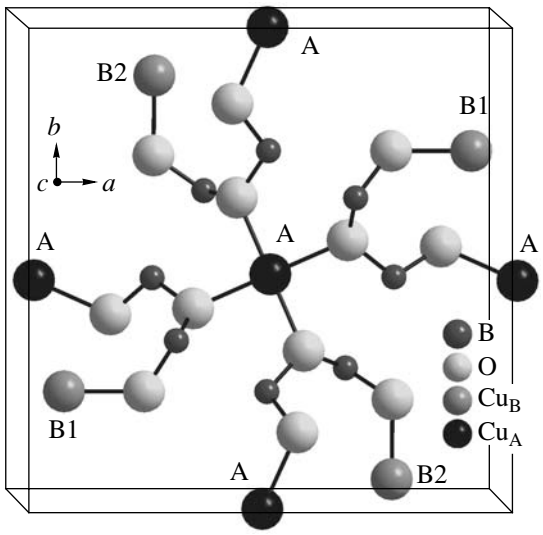

Fig. 2. Exchange between the spins of subsystem A and exchange between spins A and B (B1 and B2) nearest along the tetragonal axis.

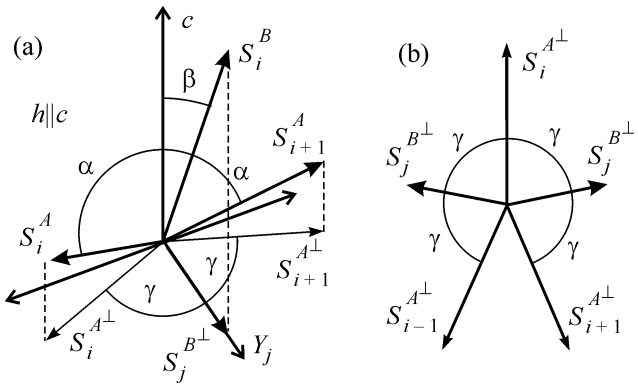

Fig. 3. Local orientation of the (a) spins in space and (b) their projections on the (x_j, y_j) plane.

angles (see Fig. 3): angles α and β between the external field applied along the tetragonal axis **c** and spins $\mathbf{S}^A$ and $\mathbf{S}^B$, respectively, and the angle γ between their projections onto the tetragonal plane. All the spins of each subsystem are in the same local environment.

The minimization of the free energy with the angles α, β, and γ of the equilibrium orientation of the spins is performed in the molecular-field approximation. For one spin $\mathbf{S}^A$ and two spins $\mathbf{S}^B$ ($S = 1/2$),

$$F = -T \ln Z_{1+2} = -T(\ln(\exp(h_a/2T) + \exp(-h_a/2T)) + 2\ln(\exp(h_b/2T) + \exp(-h_b/2T))), \quad (4)$$

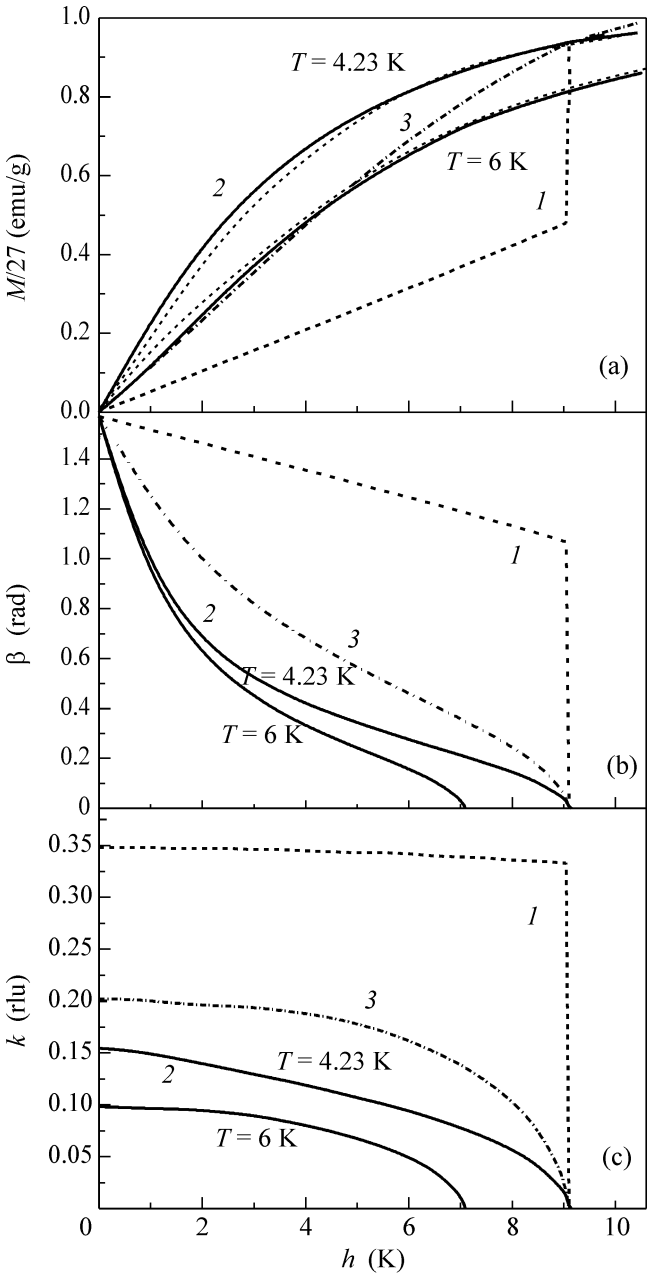

Fig. 4. Field dependence of the (a) magnetization, (b) orientation of the moments of subsystem B, and (c) wave vector of the helicoid. The points are the experimental data, dotted line *1* is the competing exchange model, solid lines *2* correspond to the frustration model, and dash–dotted line *3* is the paramagnetic case.

where

$$h_a = h\cos\alpha - 2J^A S_a(\cos^2\alpha + \sin^2\alpha\cos 2\gamma) - J_1^{AB} S_b(\cos\alpha\cos\beta + \sin\alpha\sin\beta\cos\gamma) - J_2^{AB} S_b(\cos\alpha\cos\beta + \sin\alpha\sin\beta\cos 3\gamma) - J_3^{AB} S_b(\cos\alpha\cos\beta + \sin\alpha\sin\beta\cos 5\gamma),$$

$$h_b = h\cos\beta - 2J_1^B S_b(\cos^2\beta + \sin^2\beta\cos 4\gamma) - 2J_2^B S_b(\cos^2\beta + \sin^2\beta\cos 8\gamma) - J_1^{AB} S_a(\cos\alpha\cos\beta + \sin\alpha\sin\beta\cos\gamma) - J_2^{AB} S_a(\cos\alpha\cos\beta + \sin\alpha\sin\beta\cos 3\gamma) - J_3^{AB} S_a(\cos\alpha\cos\beta + \sin\alpha\sin\beta\cos 5\gamma),$$

and S_a and S_b are the average spins in each subsystem. The exchange value $J_a = 45$ K in subsystem A was taken from the analysis of the spin-wave spectrum obtained from the inelastic neutron scattering experiment [17]. According to the analysis of the data on elastic neutron scattering [9], subsystem A in the temperature interval $T \sim 4$–6 K under consideration is close to saturation and the S_a value can be taken as constant: $S_a = 0.475$. The mean value of the spin S_b is determined self-consistently:

$$S_b = \frac{1}{2}\tanh\frac{h_b}{2T}. \quad (5)$$

The angles α and β obtained by numerically minimizing the free energy given by Eq. (4) under condition (5) are used to calculate the longitudinal magnetization

$$M = S_a\cos\alpha + 2S_b\cos\beta. \quad (6)$$

The angle γ determines the wave vector of the helix $k(rlu) = 2 - 4\gamma/\pi$.

The magnetization of the CuB_2O_4 single crystal is measured by the current-shell method using an automatic vibration magnetometer with a superconducting solenoid [18] in a field up to 80 kOe. The error in the measurement of the magnetic moment does not exceed 10^{-4} G cm^3, which corresponds to 3×10^{-3} G cm^3/g ≈ 10^{-4} μ_B per Cu atom for the magnetization of the CuB_2O_4 crystal with $m = 31$ mg. The temperature measurement error does not exceed 0.15 K. The orientation and fixation of the crystal on the quartz substrate with an accuracy of 1°–2° with the axis $c \parallel h$ are performed visually using a natural facet preliminarily tested by x-ray diffraction measurements.

The exchange parameters are determined by comparing magnetization (6) with the normalized experimental data at $T = 4.23$ K and $h > 5$ K (see Fig. 4a). The exchange values thus obtained are used for test comparison with the magnetization at $T = 6$ K. For convenient comparison of the Zeeman energy with the exchange values and temperature, the field is given in Kelvin degrees (1 K = 7400 Oe). The critical field at this temperature is $h_c \approx 9.1$ K. The magnetization is normalized to the saturation magnetization for subsystem B, M_0^B = 27 emu/g and, at $h > h_c$, is a superposition of the contribution from the antiferromagnetic subsystem A close to the linear and quasi-parametric contribution from subsystem B, which is also close to saturation in these

fields. When $h > h_c$, $\beta = 0$ and subsystem B is in the collinear phase and is aligned with the external field. Comparison with the experimental magnetization in this phase provides the ferromagnetic sign of the total exchange in subsystem B. Below the critical field, the field dependences of the orientation of moments B (see Fig. 4b) and, correspondingly, of the total magnetization are qualitatively different for different models of formation of the incommensurate magnetic structure. Lines *1* correspond to the model of competing exchanges of the first and second coordination spheres in the chains of subsystem B with the parameters $J_1^B = -34.3$ K, $J_2^B = 23.8$ K, $J_1^{AB} = 3$ K, and $J_2^{AB} = J_3^{AB} = 0$. The transition to the incommensurate magnetic structure with decreasing the field is stepwise: the moments of subsystem B are reoriented to the angular phase. The vector of the incommensurate magnetic structure $\mathbf{k} \neq 0$ also appears stepwise (see Fig. 4c). Thus, the field dependence of the longitudinal magnetization of CuB_2O_4 indicates that this mechanism of forming the incommensurate magnetic structure is not implemented in the copper metaborate. Lines *2* correspond to the field dependences of the magnetization, angle β, and the vector of the incommensurate magnetic structure in the model of frustrated intersubsystem exchanges: $J_1^B = -7$ K, $J_2^B = -3.5$ K, $J_1^{AB} = 4.05$ K, $J_2^{AB} = -3.85$ K, and $J_3^{AB} = 2.8$ K. In this case, a smooth change in the total magnetization with a small break in the critical field h_c holds. As the field decreases, the wave vectors of the helix for both temperatures increase smoothly to the values close to the experimental values $k_0^{\exp}(4.23\text{ K}) \approx 0.14 rlu$ and $k_0^{\exp}(6\text{ K}) \approx 0.1 rlu$ in zero field $h = 0$ [7]. The angle β between the tetragonal axis and direction of the mean moments at sites B increases smoothly to $\pi/2$; i.e., the moments lie in the basal plane. Thus, the mechanism of forming the incommensurate magnetic structure owing to the existence of frustrated intersubsystem exchanges provides good quantitative agreement with the experimental data both on the longitudinal magnetization and on the vector of the incommensurate magnetic structure.

An important difference between the exchange and relativistic mechanisms is that the threshold condition for the appearance of the incommensurate magnetic structure exists for the former mechanism and is absent for the latter mechanism. In the presence of frustrated intersubsystem exchanges, the canted antiferromagnetic sublattices in subsystem A and the appearance of the projection $S_b^\perp$ of the moments of subsystem B onto the basal plane reduce the energy proportionally to $J_l^{AB} S_a^\perp S_b^\perp \cos(2l-1)\gamma$; in the long-wavelength limit ($\delta = \pi/2 - \gamma \longrightarrow 0$), this value is always larger than the loss in the exchange energy of subsystem A ~ $J^A S_a^\perp S_a^\perp \cos 2\gamma$. Thus, the cant of the moments appears without any threshold condition on the intersubsystem exchange but under the condition of the appearance of the transverse components of the moments in subsystem B. This property gives rise to close correlation between the development of the incommensurate structure and the reorientation of the moments of subsystem B from the tetragonal axis. Since the cant of the moments is possible not only in the helical structure but also in the formation of the commensurate angular phase (see Fig. 5), it is necessary to compare the energies of these two phases. In the presence of only one intersubsystem exchange with $l = 1$, the energies of these two phases are the same. The appearance of the exchange with the second nearest neighbors J_2^{AB} of the same sign reduces the energy of the commensurate phase. However, with a further increase in the second-exchange magnitude to the threshold (bifurcation) value $J_2^{AB} = J_1^{AB}$, the energy of the helical structure becomes lower; i.e., the system changes the type of the ground state. The exchange with the second nearest neighbors of the opposite sign always stabilizes the helicoid. The transverse components of the magnetic moments of different chains of subsystem B in the helical phase with respect to each other are locally oriented antiferromagnetically. This gives rise to the appearance of the Lifshitz invariant in the thermodynamic potential density:

$$\frac{d\Phi_L}{dV} = C\left(l_b \frac{\partial l_a}{\partial z} - l_a \frac{\partial l_b}{\partial z}\right), \qquad (7)$$

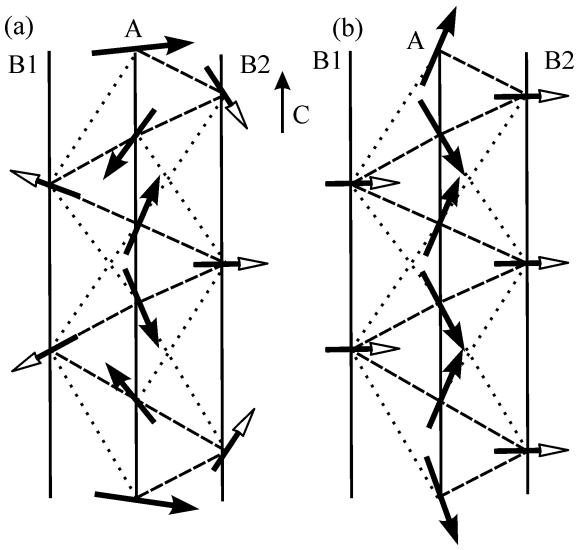

Fig. 5. Removal of the degeneration of (a) helical and (b) commensurate structures owing to (dotted lines) the exchange between the second nearest neighbors. The moment projections on the basal plane are shown.

where, in contrast to [10], the two-component order parameters responsible for the appearance of the helical structure are the transverse antiferromagnetism vectors l_a and l_b of subsystems A and B. The derivation of this invariant, as well as the detailed analysis of the effect of interactions in subsystem B on the threshold conditions, will be presented in a forthcoming publication. We only note that this invariant absent in the model of competing exchanges appears in our case due to the frustrated intersubsystem bonds. The ferromagnetic interaction inside the chains does not change the boundary conditions, whereas the exchange between the chains stabilizes either the helix or the angle phase. Figure 4 demonstrates the possibility of the appearance of the helical structure in the paramagnetic case (lines *3*) with the exchanges $J^B_{1,2} = 0$, $J^{AB}_1 = -2.02$ K, and $J^{AB}_2 = -12.5$ K. The exchange values are chosen so that the transition to the helical phase occurs at the same point of the phase diagram and with the same magnetization value as in CuB_2O_4. This example shows that the isotropic "paramagnetic" subsystem can give rise to the qualitative rearrangement of the exchange-ordered subsystem in the presence of intersubsystem frustration even in the absence of proper exchange interactions.

In addition to interest for pure magnetic transitions, the mechanism of formation of the incommensurate magnetic structure is of fundamental importance for describing magnetoelectric effects (see, e.g., the review of multiferroics in [19] and works [20, 21]), where the frustrated exchange interactions are of key importance for the appearance of the electric polarization. Copper metaborate (CuB_2O_4) is the first of the two-subsystem antiferromagnets under investigation in which the incommensurate magnetic structure is formed due to the removal of frustration in intersubsystem exchange interaction.

We are grateful to A.I. Pankrats for stimulating discussions.

REFERENCES

1. M. F. Collins and O. A. Petrenko, Can. J. Phys. **75**, 605 (1997).
2. H. Kawamura, J. Phys.: Condens. Matter **10**, 75111 (1998).
3. V. P. Plakhty, J. Kulda, D. Wisser, et al., Phys. Rev. Lett. **85**, 3942 (2000).
4. G. Petrakovskii, D. Velikanov, A. Vorotinov, et al., J. Magn. Magn. Mater. **205**, 105 (1999).
5. G. A. Petrakovskiĭ, M. A. Popov, B. Roessli, and B. Ouladdiaf, Zh. Éksp. Teor. Fiz. **120**, 926 (2001) [JETP **93**, 809 (2001)].
6. B. Roessli, J. Schefer, G. Petrakovskii, et al., Phys. Rev. Lett. **86**, 1885 (2001).
7. G. A. Petrakovskiĭ, A. I. Pankrats, M. A. Popov, et al., Fiz. Nizk. Temp. **28**, 840 (2002) [Low Temp. Phys. **28**, 606 (2002)].
8. A. I. Pankrats, G. A. Petrakovskiĭ, M. A. Popov, et al., Pis'ma Zh. Éksp. Teor. Fiz. **78**, 1058 (2003) [JETP Lett. **78**, 569 (2003)].
9. M. Boehm, B. Roessli, J. Schefer, et al., Phys. Rev. B **68**, 024405 (2003).
10. M. A. Popov, G. A. Petrakovskiĭ, and V. I. Zinenko, Fiz. Tverd. Tela (St. Petersburg) **46**, 478 (2004) [Phys. Solid State **46**, 484 (2004)].
11. A. Pankrats, G. Petrakovskii, V. Tugarinov, et al., J. Magn. Magn. Mater. **300**, e388 (2006).
12. Yu. A. Izyumov, *Diffraction of Neutrons on Long-Period Structures* (Énergoatomizdat, Moscow, 1987), p. 143 [in Russian].
13. I. E. Dzyaloshinskiĭ, Zh. Éksp. Teor. Fiz. **47**, 992 (1964) [Sov. Phys. JETP **20**, 665 (1964)].
14. S. Martynov, G. Petrakovskii, and B. Roessli, J. Magn. Magn. Mater. **269**, 106 (2004).
15. S. N. Martynov, Fiz. Tverd. Tela (St. Petersburg) **47**, 654 (2005) [Phys. Solid State **47**, 678 (2005)].
16. M. Martinez-Ripoli, S. Martinez-Carrera, and S. Carcia-Blanco, Acta Crystallogr. B **27**, 677 (1971).
17. M. Boehm, S. Martynov, B. Roessli, et al., J. Magn. Magn. Mater. **250**, 313 (2002).
18. A. D. Balaev, Yu. B. Boyarshinov, M. M. Karpenko, and B. P. Khrustalev, Prib. Tekh. Éksp., No. 3, 167 (1985).
19. S.-W. Cheong and M. Mostovoy, Nature Mater. **6**, 13 (2007).
20. M. Mostovoy, Phys. Rev. Lett. **96**, 067601 (2006).
21. I. A. Sergienko and E. Diagotto, Phys. Rev. B **73**, 094434 (2006).

Translated by R. Tyapaev